PERGAMON

International Journal of Heat and Mass Transfer 42 (1999) 1255–1272

International Journal of HEAT and MASS TRANSFER

Single-phase heat transfer enhancement in a curved, rectangular channel subjected to concave heating

J. Christopher Sturgis[1], Issam Mudawar*[,2]

Boiling and Two-Phase Flow Laboratory, School of Mechanical Engineering, Purdue University, West Lafayette, IN 47907, U.S.A.

Received 12 February 1998; in final form 17 July 1998

Abstract

Experiments were performed to ascertain the single-phase heat transfer enhancement provided by streamwise curvature. Curved and straight rectangular flow channels were fabricated with identical 5.0×2.5 mm cross-sections and 101.6 mm heated lengths in which heat was applied to a 32.3 mm radius concave wall in the curved channel and a side wall in the straight. Reynolds number ranged from 9000 to 130 000 and centripetal acceleration for the curved flow reached 315 times the earth's gravitational acceleration. Nusselt numbers defined with hydraulic and thermal diameters were consistently underpredicted by previous correlations developed for full-periphery-heated channels but were accurately predicted when defined with heated width. Convection coefficients were enhanced due to flow curvature for all conditions tested, and detailed experimental correlations are provided for both the straight and curved configurations. Increasing Reynolds number produced different enhancement trends for different locations along the heated wall, decreasing the enhancement near the inlet and increasing it elsewhere downstream. Mechanisms responsible for the curvature enhancement are believed to be Dean vortices and a shift in the maximum axial velocity toward the concave wall. These mechanisms require a finite distance to develop sufficient strength to influence heat transfer, which explains the different enhancement trends observed for different locations along the heated wall.

Nomenclature

A channel cross-sectional area
C_1, C_2 constants in eqn (1)
C_3, C_4 constants in eqn (2)
D geometric diameter of tube
d_c curvature diameter
D_e Dean number
D_h hydraulic diameter of channel $[4A/P_w]$
D_{th} thermal diameter of channel $[4A/P_h]$
f friction factor
g^* centripetal acceleration normalized with respect to earth's gravitational acceleration
g_e earth's gravitational acceleration
H channel height
h heat transfer coefficient
k fluid thermal conductivity
L1, L2 Location 1, Location 2, ..., thermocouple locations in heater
L_q length of discrete heater (streamwise direction)
$\underline{Nu}$ Nusselt number
Nu Nusselt number averaged over channel perimeter
P_h heated perimeter
P_o pressure at outlet of heated length
Pr Prandtl number
P_w wetted perimeter
q'' heat flux
Re_D Reynolds number based on diameter (geometric or hydraulic)
r radial coordinate in curved heater
R_1 inner wall radius of curved channel
R_2 outer wall radius of curved channel
T temperature
T_b bulk fluid temperature
T_{in} fluid inlet temperature

* Corresponding author. Tel.: +1 765 494 5705; fax: +1 765 494 0539; e-mail: mudawar@ecn.purdue.edu
[1] Graduate student.
[2] Professor and Director of the Purdue University Boiling and Two-Phase Flow Laboratory.

0017–9310/98/$ - see front matter
PII: S0017–9310(98)00232–4

T_w wall temperature
U mean velocity
u_{axial} local value of axial velocity in channel
W channel width
W_q width of discrete heater (perpendicular to flow direction)
x transverse coordinate in straight heater [$x = 0$ at fluid–surface interface]
z streamwise coordinate [$z = 0$ at heater inlet].

Greek symbols
ν kinematic viscosity
μ dynamic viscosity
θ turn angle of flow, measured from beginning of curvature.

Subscripts
cr transition from laminar to turbulent flow
cur curved channel/heater
D geometric or hydraulic diameter
H channel height
L heated length
str straight channel/heater
th thermal
W heated width
w wall.

1. Introduction

Numerous applications involve heat transfer to a fluid flowing through a curved passage. For example, the coolant channels at the throat of a rocket engine, Fig. 1(a), and the receiver coil of a solar power generation system both exhibit streamwise curvature, with the additional characteristic of one-sided heating. Of particular interest to the present study are those passages which have rectangular cross-sections since they may be milled into a substrate and assume a greater variety of shapes than tubes. In this way, they may be tailored to a variety of heat transfer applications. While many researchers have focused efforts on the heat transfer characteristics of tubular configurations, the authors of the present study have found relatively little work that addresses the heat transfer enhancement associated with the combination of streamwise curvature, rectangular cross-section and concave heating, as depicted in Fig. 1(b). Therefore, the present experimental study was initiated to more closely investigate the single-phase heat transfer characteristics of this geometry.

Streamwise curvature has been shown to enhance single-phase heat transfer, yet data indicating such effects are associated mostly with circular tubes. Seban and McLaughlin [1] noted this enhancement in their work with full-periphery-heated coil tubes. They used perimeter-averaged convection coefficients in their correlations even though they noted in some cases convection coefficients varied by as much as a factor of four about the perimeter. Rogers and Mayhew [2] and Pratt [3] also demonstrated the enhancement of heat transfer using coiled tubes.

Considering rectangular cross-sections, McCormack et al. [4] heated only the concave wall of a large width-to-depth ratio duct achieving Nusselt number increases of 30–190% over that of a straight duct. The aspect ratio of their curved duct allowed for the formation of multiple pairs of counter-rotating vortices. Dement'eva and Aronov [5] examined flow in curved, rectangular channels in which heat transfer was from the fluid (hot air) to the walls. Chung and Hyun [6] numerically investigated laminar flow in a rectangular channel with concave heating. They showed that the hydrodynamics begin to influence heat transfer beyond a certain point downstream of the initial curvature.

Certain test conditions need to be considered when applying the results of these investigations. First is the extent of the cross-section over which heat is applied. The secondary flows established in the cross-section have a particular orientation with respect to the radius of curvature. Therefore, the relationship between the hydrodynamics and heat transfer is different for concave, full-periphery and convex heating.

Secondly, the geometry of the cross-section can be consequential. Employing the definition of hydraulic diameter allows for the comparison of circular and rectangular cross-sections. Collier and Thome [7] indicated that single-phase convection correlations developed for tubes may be applicable to rectangular channels for cases in which the entire parameter is heated, and Kays and Perkins [8] suggested that the errors introduced in doing so are small for turbulent flow. However, round tube correlations may be inaccurate when there is asymmetric heating. Also, thermal boundary layer development and attainment of thermally fully-developed conditions may be altered with asymmetric heating.

Thirdly, the flow condition has a strong bearing on the heat transfer characteristics of a curved channel. Turbulent flow has greater diffusive properties, flatter velocity profiles and larger wall shear stresses as well as stronger secondary motions associated with curvature [9].

Additionally, the streamwise extent of the heated region affects the applicability of correlations. For a short heater, a larger percentage of its length may fall within the thermally-developing region where the convection coefficient is relatively large. Therefore, correlations developed under these conditions may not be accurate when applied to longer heaters where a substantial fraction of the heated length is within the thermally fully-developed region [10].

The results of the aforementioned investigations have certain limitations when considering the present con-

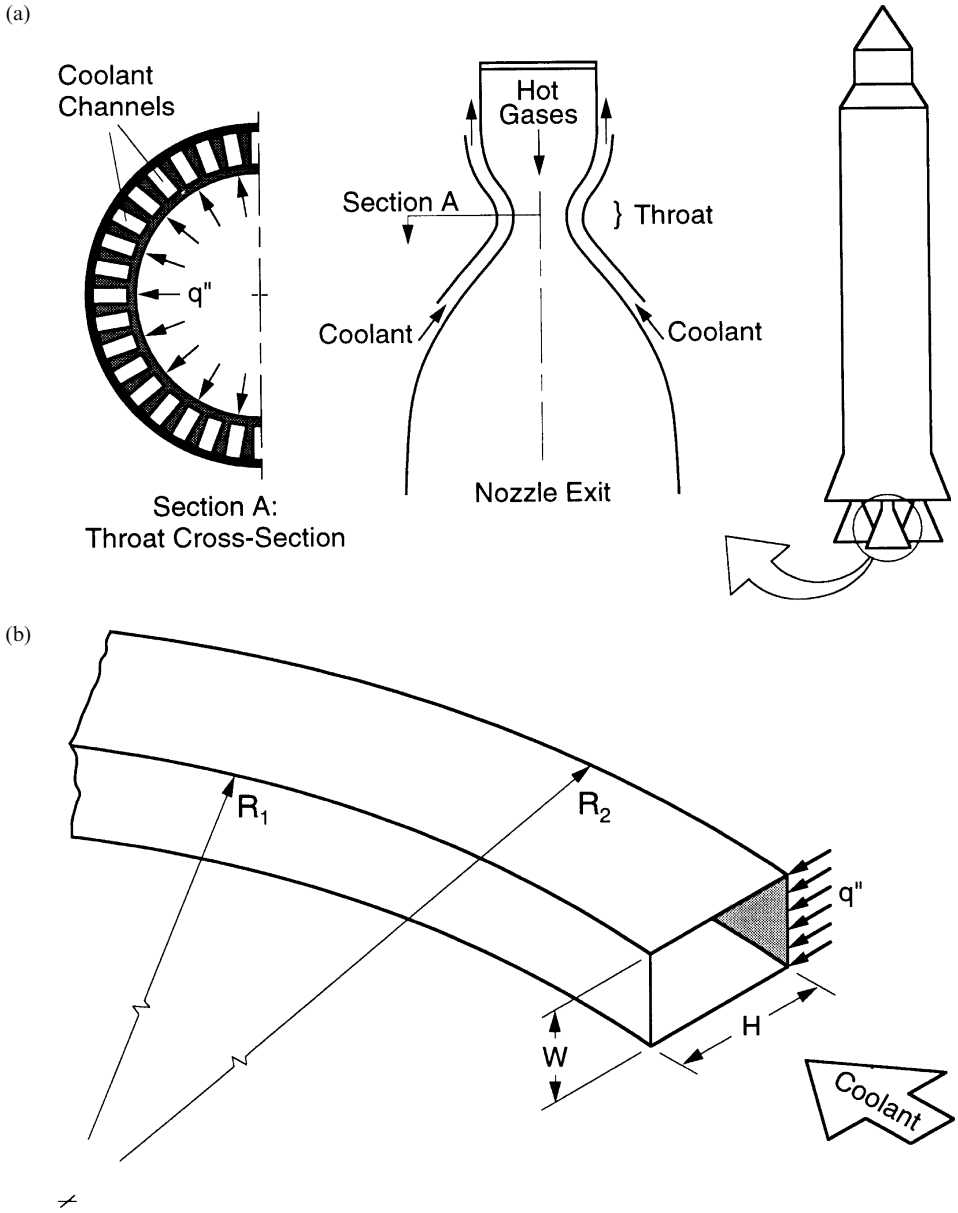

Fig. 1. Flow in a curved, rectangular channel subjected to concave heating as it exists in (a) the cooling circuit of a rocket engine and (b) the present study.

figuration of interest because of the unique hydrodynamic and thermal characteristics it presents. This configuration concerns heat transfer to a turbulent flow of liquid in a curved, rectangular channel subjected only to concave heating over a relatively long length. In the present study, the same test matrix was repeated for a straight channel in order to assess the enhancement for which curvature is responsible. In this manner, the curvature enhancement effect could be isolated and quantified.

2. Experimental methods

2.1. Experimental apparatus

Two channel designs were tested as part of this research—a curved and a straight channel. Each had a 5.0×2.5 mm cross-section which was milled into a plate of high-temperature G-10 fiberglass plastic. The channel was formed when a second G-10 plate was placed atop the first as shown in Fig. 2 for the curved channel;

assembly of the straight channel was similar. The heater was inserted as shown in Fig. 2 and aligned with the aid of a microscope so that it was flush with the interrupted wall. The heated surface in the curved channel was the concave wall (32.3 mm radius) and in the straight channel a side wall. Fluid temperature and pressure were measured just upstream and downstream of the heated section. The two flow channels were therefore nearly identical, having the same cross-section, hydrodynamic entry length (106 hydraulic diameters), heated wall (2.5×101.6 mm), thermocouple locations, flow instrumentation and material with the only significant difference being the curvature of the heated section.

The curved and straight heaters are shown in Fig. 3(a) and (b) respectively. Both heaters were made from 99.99% pure oxygen-free copper. To determine local wall flux and wall temperature, a set of three Type-K thermocouples was positioned normal to the heated wall at each of five locations in each heater as illustrated in Figs. 3 and 4. Corresponding locations in each were the same distance from the inlet with the inlet set designated as Location 1 (L1) and the outlet set as Location 5 (L5). The thermocouple beads were epoxied into three small holes that were precisely drilled with respect to each other and the heated wall. Power was supplied by cylindrical cartridge heaters embedded in the thick portions of each heater as indicated in Fig. 4. The set of five cartridge heaters in the curved channel and four in the straight were connected to a 240-volt variac allowing power to be carefully incremented during testing. Distributing the cartridge heaters symmetrically as shown and using copper for construction of the heater blocks helped ensure even power distribution along each heated length.

Each assembled flow channel was tested using the flow loop shown schematically in Fig. 5. A centrifugal pump circulated fluid through the main and test section subloops and the indicated components. Fluid temperature was controlled by an immersion heater submerged in the loop reservoir and by a series of flat-plate heat exchangers. The fluid selected for this investigation was FC-72, a dielectric Fluorinert manufactured by 3M Company.

2.2. Data reduction

Assuming one-dimensional conduction through the thin, instrumented portion of each copper heater, a temperature profile was calculated based on the three readings from a set of thermocouples. A least-squares best-fit analysis was used to determine the logarithmic profile in the curved heater and linear profile in the straight heater, which are given, respectively, by

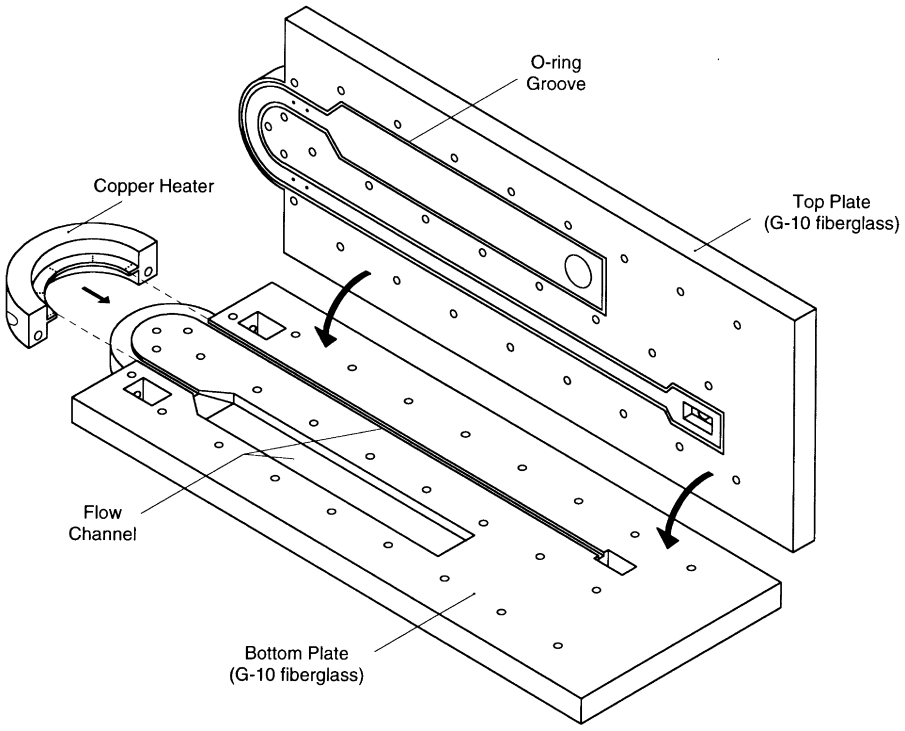

Fig. 2. Assembly view of curved channel showing heater and G-10 fiberglass plates.

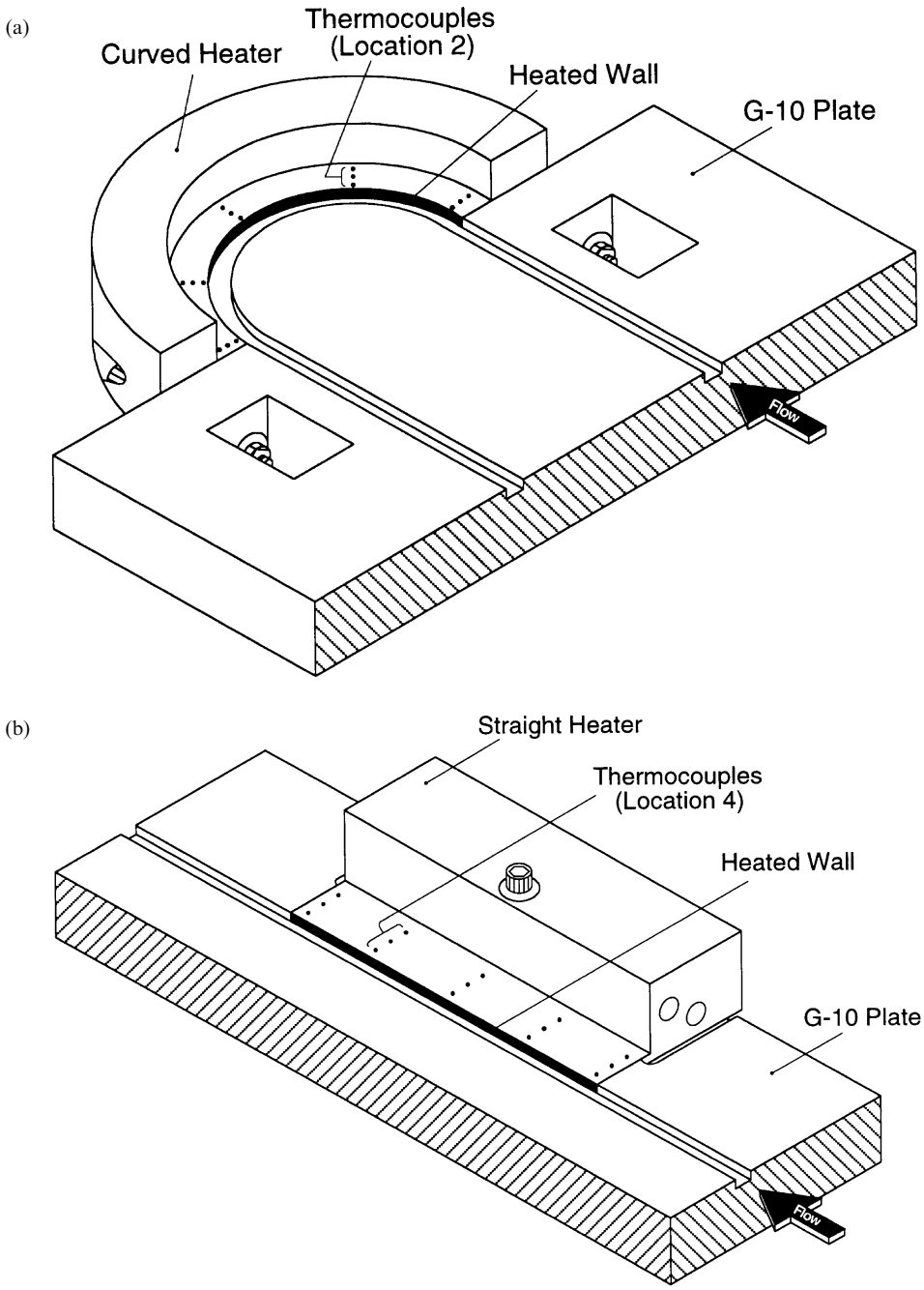

Fig. 3. (a) Curved and (b) straight heaters inserted into their respective channels. Hydrodynamic entry length is not shown.

$$T(r) = C_1 \ln\left(\frac{r}{R_2}\right) + C_2 \quad (1)$$

and

$$T(x) = C_3 x + C_4, \quad (2)$$

where $r = R_2$ indicates the concave heated wall and $x = 0$ the straight heated wall. These profiles were used to calculate both the wall heat flux, q'' (assuming a constant copper conductivity of 391 W m^{-1} K^{-1}), and wall temperature, T_w.

Fluid bulk temperature, T_b, at each location along each channel was calculated based on the heat input up to

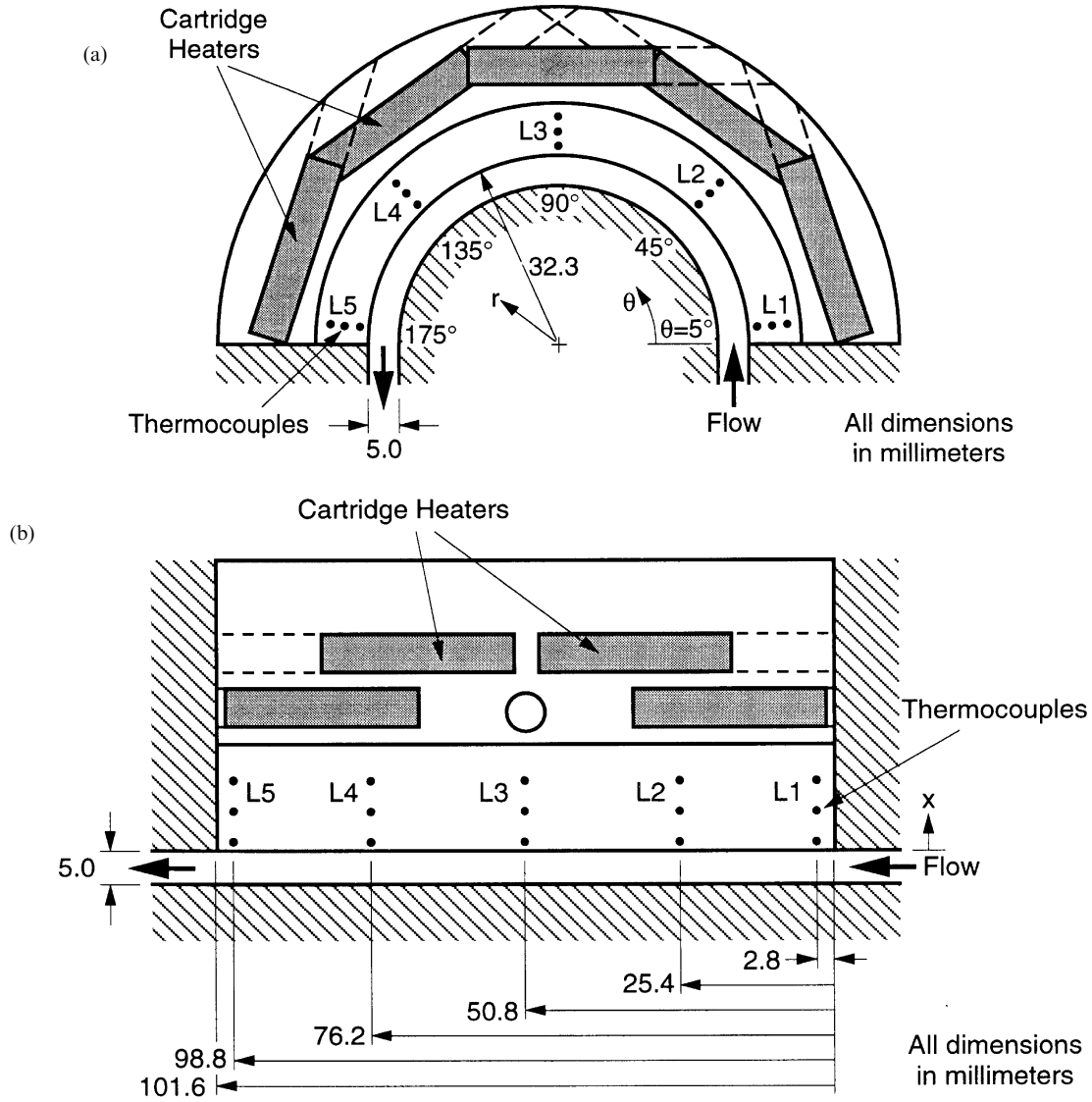

Fig. 4. Top view of (a) curved and (b) straight heaters illustrating locations of thermocouples and cartridge heaters.

that location and the assumption of a well-mixed flow. Considering the secondary flows associated with turbulence and curvature, this assumption is quite reasonable for single-phase flow.

The local convection coefficient, h, was defined by the temperature difference between the heated wall and fluid,

$$h \equiv \frac{q''}{T_w - T_b} \tag{3}$$

Channel outlet pressure, P_o, was held constant at 1.38 bar for all the data. P_o was defined as the pressure at the end of the heated section, which varied slightly from that measured at the pressure tap placed a short distance downstream of the heated section. The frictional losses incurred between these two locations were estimated (losses were linear with respect to length) then added to the measured value to determine P_o.

2.3. Test conditions

Fully-developed turbulent flow existed at the heater inlet for all data reported here since the Reynolds number based on hydraulic diameter, $Re_D = UD_h/v$, was greater than 9000 and the hydrodynamic entry length measured over 100 hydraulic diameters. Ito [11] noted that the critical Reynolds number marking transition to turbulent flow is greater for curved flow than straight and offered the following criterion for assessing flow conditions,

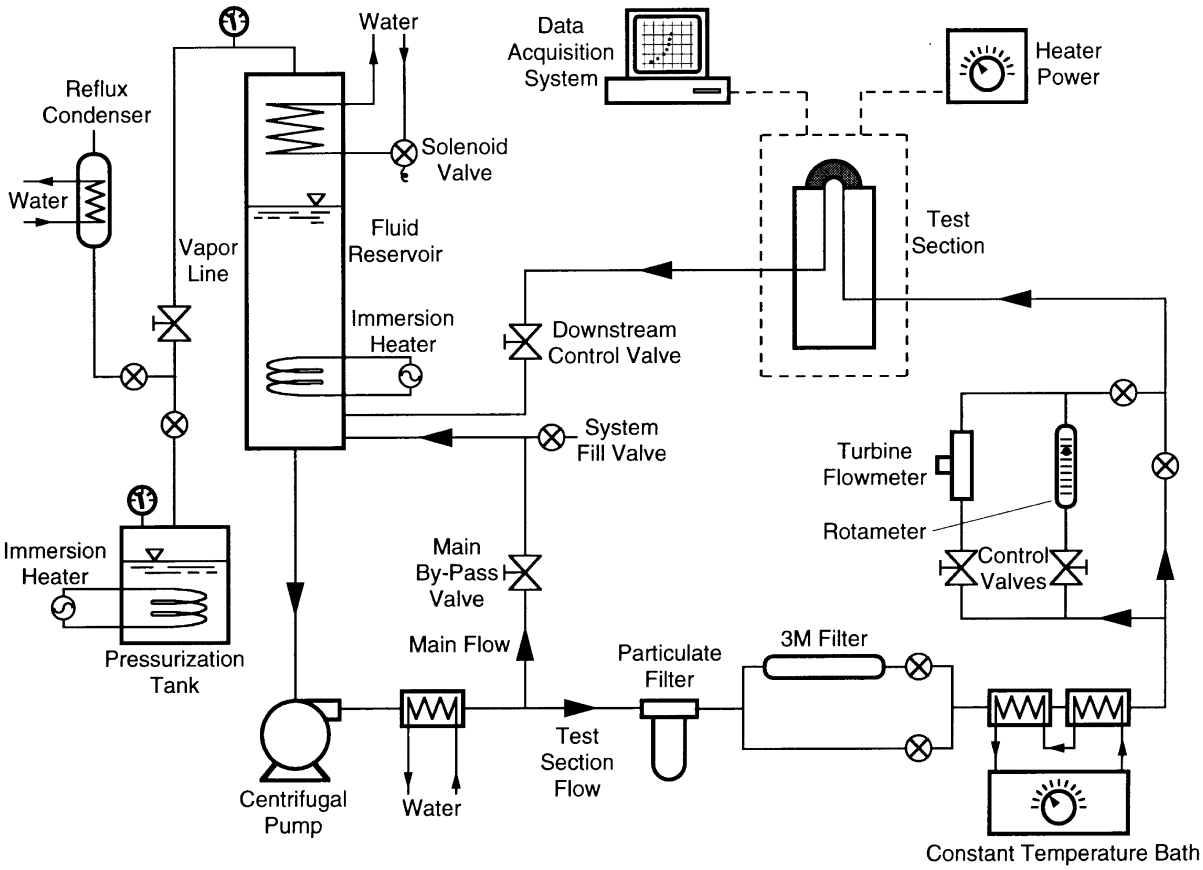

Fig. 5. Flow loop and auxiliary components.

$$Re_{D,\mathrm{cr}}|_{\mathrm{cur}} = 2\left(\frac{D_h}{2R_2}\right)^{0.32} \times 10^4 \tag{4}$$

which is applicable for

$$15 < \frac{2R_2}{D_h} < 860. \tag{5}$$

For the curved geometry of the present investigation, $Re_{D,\mathrm{cr}}|_{\mathrm{cur}} = 7800$. Therefore, flow conditions were considered fully-turbulent for curved flow as well. Definitions and ranges of key parameters are given in Table 1. Unless otherwise noted, all fluid properties were evaluated at the local bulk temperature.

2.4. Repeatability and uncertainty analysis

The procedures for assembling the channel and acquiring data were consistent throughout the tests. Data from duplicate tests were nearly identical indicating repeatable results, negligible aging of the channel and consistent assembly procedures. Uncertainty in heat flux was approximately 8.5% at low fluxes ($q'' \approx 30$ W cm^{-2}) and smaller for higher high fluxes. Wall temperature calculations were accurate to within 0.3°C and flowrate uncertainty was less than 2.3%. In regards to correlations presented in the next sections, the Reynolds and Nusselt numbers defined with respect to hydraulic diameter, Re_D and Nu_D, were accurate to within 3 and 8%, respectively. Heat loss from the large, exposed faces of the copper heater block was not of concern since heat flux was not derived from electrical power input but rather the temperature profile based on thermocouple readings. Numerical modeling revealed the losses from the thin, instrumented segment represented only about 5% of the heat flowing into this segment for low fluxes ($q'' \approx 15$ W cm^{-2}) and even smaller for high fluxes.

3. Experimental results

3.1. Straight channel

Straight channel tests were conducted over a broad range of flow velocity ($U = 1$–10 m s^{-1}). The convection

Table 1
Definitions and ranges of key parameters

Parameter	Variable	Range
Mean velocity	U	1.0–10.0 m s^{-1}
Inlet temperature	T_{in}	30–62°C
Pressure at outlet of heater	P_o	1.38 bar (constant)
Convection coefficient	$h = q''/(T_w - T_b)$	2000–20 800 W m^{-2} K^{-1}
Reynolds number	$Re_D = UD_h/v$	9000–130 000
Prandtl number	Pr	8.5–11.2
Nusselt number	$Nu_D = hD_h/k$	110–1340
Viscosity ratio	μ/μ_w	1.03–1.33
Dean number	$De = Re_D\sqrt{D_h/(2R_2)}$	450–29 600
Centripetal acceleration	$g^* = U^2/(g_e R_2)$	3–315

coefficient, h, in all tests increased with increasing velocity and initially decreased with streamwise distance before reaching an asymptotic value.

The convection coefficients calculated with local values (eqn (3)) were used to define Nusselt numbers,

$$Nu_D = \frac{hD_h}{k}, \tag{6}$$

which were correlated with local Reynolds and Prandtl numbers.

The extent of the thermal entrance region was ascertained by plotting Nu_D against z/D_h, the streamwise distance non-dimensionalized by the hydraulic diameter. This is shown in Fig. 6 for $T_{in} = 45$–49°C at select velocities with the z/D_h values corresponding to the locations at which thermocouples were placed in the straight heater. For each velocity indicated, the Nusselt numbers at $z/D_h = 0.8$ (Location 1) are consistently higher than downstream values, while Nu_D for $z/D_h = 7.5$, 15 and 29.2 (corresponding to Locations 2, 3 and 5) have approximately the same value as indicated by the horizontal-line fit. The values at $z/D_h = 22.5$ are not shown due to difficulties with thermocouples at Location 4. Constant values of Nu_D for $z/D_h \geqslant 7.5$ indicate that thermal conditions are fully-developed over this region and it is appropriate to use these single-phase data points in developing a thermally fully-developed correlation. Hartnett [12] showed that turbulent heat transfer coefficients for full-periphery-heated pipes decrease to asymptotic values around $z/D = 10$–15 and Kays and Crawford [13] presented analytical solutions with similar conclusions for $Pr \approx 10$. It appears the extent of the thermal entrance region, measured in hydraulic diameters, is similar for one-side-heated channels (present study) and full-periphery-heated tubes.

Having identified the thermally fully-developed region, a correlation was developed from all data at Locations 2, 3 and 5. A least-squares method was employed to fit these 1668 data points with a power-law function, resulting in the following correlation

$$Nu_D = 0.0306 Re_D^{0.808}\, Pr^{0.4} \tag{7}$$

which has a mean absolute error of 3.5%. All properties were evaluated at the local bulk temperature and the exponent on Pr was set equal to 0.4 (typical for turbulent flow) since the relatively small range of Prandtl number tested in the present study precluded any accurate determination of this exponent.

Equation (7) was compared with the well-known correlation of Dittus and Boelter [14],

$$Nu_D = 0.023 Re_D^{0.8}\, Pr^{0.4} \tag{8}$$

recommended for full-periphery heated tubes. Figure 7 shows that the Dittus–Boelter correlation underpredicts the present one-side-heated channel data by an average of 31% though the slopes (on a log–log plot) are nearly identical.

For large wall-to-fluid temperature differences, cross-stream and axial viscosity gradients exist in the fluid which affect the velocity gradient at the wall and the local Reynolds number, both of which influence the heat transfer coefficient [15]. Incorporating the ratio of fluid viscosity evaluated at the local bulk and local wall temperatures, all the present thermally fully-developed data points were also correlated by

$$Nu_D = 0.0333 Re_D^{0.811}\, Pr^{1/3} \left(\frac{\mu}{\mu_w}\right)^{0.14} \tag{9}$$

with a slightly lower mean absolute error of 3.2% and all properties, except μ_w, evaluated at the local bulk temperature. The Prandtl number and viscosity ratio exponents were chosen in accordance with the commonly-used Sieder–Tate [16] correlation. Their correlation, developed from full-periphery-heated tube data, underpredicts the present data by an average of 29%.

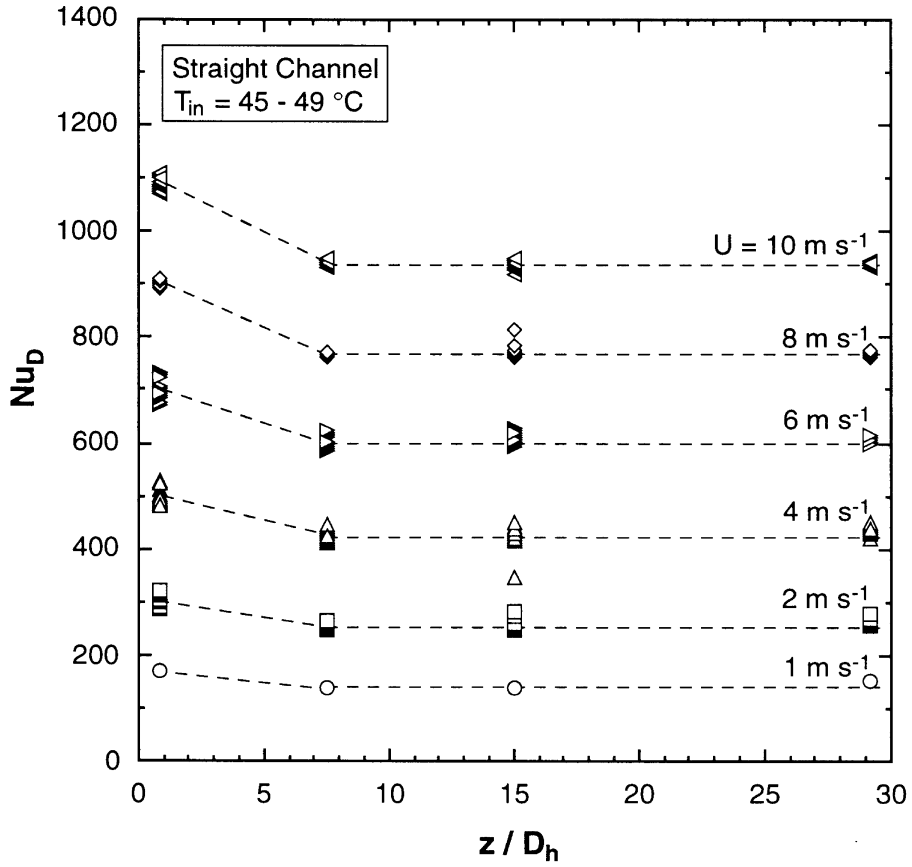

Fig. 6. Nusselt number variation along heated wall in straight channel.

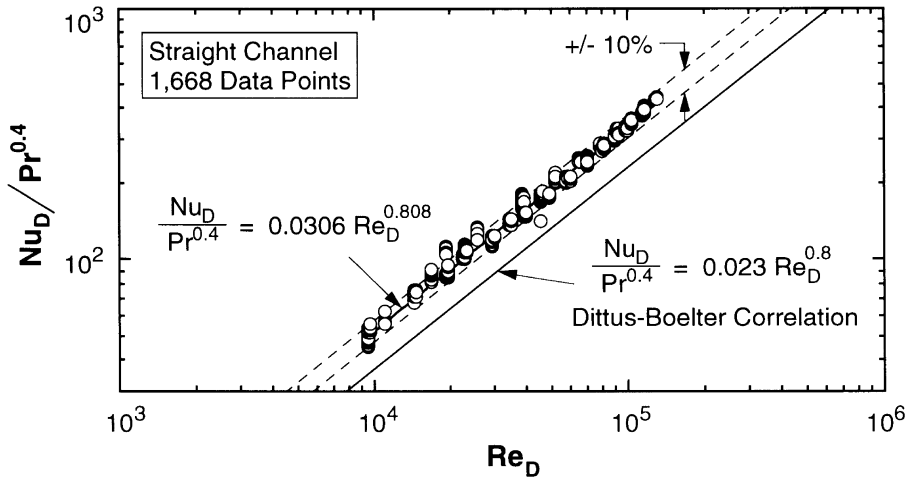

Fig. 7. Data and correlation for present straight, one-side-heated channel compared with Dittus–Boelter correlation [14] for straight, full-periphery-heated tubes.

Table 2 shows several published correlations for single-phase heat transfer, the conditions under which they were developed and the accuracy with which they predict the present data. None can be considered a satisfactory representation of the present data, although the correlations by Incropera et al. [18] and Maddox and Mudawar [19] yield reasonable results when recast in terms of hydraulic diameter. However, the slopes (i.e., Reynolds number exponents) of these correlations do not reflect the slope of the present data. They were developed with short, discrete heaters placed on a wall that was wider than the heated width. It can therefore be concluded that correlations developed with full-periphery-heated tubes and with short, discrete heaters do not accurately predict data obtained in long, one-side-heated rectangular channels.

Several length scales may be considered when the geometry involves a rectangular channel heated over only a portion of its perimeter. Three possible scales are the hydraulic diameter, D_h, thermal diameter, D_{th}, and heated width, W. Their definitions and values for the present work are,

$$D_h = \frac{4A}{P_w} = \frac{2HW}{H+W} = 3.4 \quad \text{mm} \tag{10}$$

$$D_{th} = \frac{4A}{P_h} = 4H = 20.3 \quad \text{mm} \tag{11}$$

$$W = 2.5 \quad \text{mm} \tag{12}$$

The hydraulic diameter is defined in terms of the wetted perimeter whereas the thermal diameter uses the heated perimeter.

Since Reynolds number is an indication of the hydrodynamic characteristics of the flow configuration and Nusselt number the thermal characteristics, the length scale used in each definition should reflect these conditions. For full-periphery-heated tubes, the proper choice in both terms is the geometric diameter, D, which is identical to the hydraulic and thermal diameters. Considering a rectangular cross-section, the appropriate and well-accepted definition of Reynolds number incorporates the hydraulic diameter, which has been employed here. Use of thermal diameter in the Nusselt number is an attempt to account for the asymmetry of the heating condition. However, redefining the 1668 data points with this length scale in the Nusselt number led to an even larger discrepancy between the data and the Dittus–Boelter correlation with the data consistently underpredicted by an average of 88%. The data were also analyzed with Nusselt number defined in terms of the heated width. Though these fall much closer to the Dittus–Boelter prediction, this is regarded merely as a consequence of the particular length scale value since the Nusselt numbers are not consistently defined. Therefore, caution must be exercised when applying a full-periphery-heating correlation (perimeter-averaged Nu) to conditions with only partial-perimeter heating (localized Nu).

These facts highlight a common problem in single-phase analysis—the selection of a correlation for convection coefficient and the interpretation of variables in the expression. This is particularly troublesome with non-circular geometry where dimensions of channel cross-section and heated surface must be considered. As mentioned earlier, the hydraulic diameter allows comparison of hydrodynamic characteristics but proper representation of thermal characteristics is often specific to test conditions. Therefore, the present work contributes a single-phase correlation for the turbulent flow of liquid through a straight, rectangular channel heated on one side, applicable under thermally fully-developed conditions. Additionally, when the heated width is used as the thermal length scale, the thermally fully-developed correlation becomes

$$Nu_w = \frac{hW}{k} = 0.0229 Re_D^{0.808}\, Pr^{0.4} \tag{13}$$

3.2. Curved channel

Heat transfer experiments conducted in the curved channel covered the same matrix of conditions as the straight channel. As with the straight channel, the convection coefficient in the curved channel increased with increasing velocity. However, plotting the Nusselt number against streamwise location did not yield the same conclusion regarding a thermally fully-developed region as did the straight channel data. Figure 8 shows Nu_D variation with z/D_h for $T_{in} = 44$–49°C and several velocities. Nu_D does not tend toward a constant value indicating that the flow did not reach a thermally fully-developed state prior to exiting the heated section. Between Locations 1 and 2, Nu_D increases or remains constant (unlike in the straight channel where it decreases) as a consequence of curvature-induced secondary flows. Location 1 is so close to the inlet that the curvature has little influence on Nu_D, as evidenced by Nusselt number values similar to those of the straight channel given in Fig. 6. Chung and Hyun [6] showed numerically for laminar flow in a curved duct that secondary flows are not of significant strength at the inlet but do influence heat transfer beyond turn angles of $\theta \geqslant 15^\circ$, measured from the beginning of curvature. The same can be expected for turbulent flow, namely, that it takes a finite distance for the secondary flows to develop and influence the heat transfer as Fig. 8 suggests. Farther downstream, Fig. 8 shows Nusselt numbers tend to rise at the exit.

Without an explicit thermally fully-developed region, correlations were determined for specific locations along the curved channel and are given in Table 3. All data at the exit of the curved section (Location 5) were correlated by

$$Nu_D = 0.0225 Re_D^{0.854}\, Pr^{0.4} \tag{14}$$

Table 2
Heat transfer correlations for flow in straight channels

Author [ref]	Published correlation (eqn)	Elaboration	Mean absolute error with respect to present data (%)
Dittus and Boelter [14]	$Nu_D = 0.023 Re_D^{0.8}\, Pr^{0.4}$	Tube with full-periphery heating; properties at bulk temperature; developed with gases; $Re_D \geqslant 10^4$; $0.7 \leqslant Pr \leqslant 160$: $T_w - T_b \leqslant 6^\circ C$.	30.7
Sieder and Tate [16]	$Nu_D = 0.027 Re_D^{0.8}\, Pr^{1/3} \left(\frac{\mu}{\mu_w}\right)^{0.14}$	Tube with full-periphery heating; properties at bulk temperature, except μ_w at T_w; developed with liquids; $Re_D \geqslant 10^4$; $0.7 \leqslant Pr \leqslant 16\,700$.	28.9
Petukhov and Popov [17]	$Nu_D = \frac{(f/8) Re_D Pr}{1.07 + 12.7(Pr^{2/3} - 1)\sqrt{f/8}}$	Tube with full-periphery heating; properties at bulk temperature; $10^4 \leqslant Re_D \leqslant 5 \times 10^6$; $0.5 \leqslant Pr \leqslant 2000$; friction factor, f, from Moody diagram or for smooth tubes, $f = [1.82 \log(Re_D) - 1.64]^{-2}$.	20.3
Incropera et al [18]	$\overline{Nu_L} = 0.13 Re_D^{0.64}\, Pr^{0.38} \left(\frac{\mu}{\mu_w}\right)^{0.25}$	Rectangular channel with short, discrete heater; properties at inlet temperature, except μ_w at T_w; developed with water and FC-77 liquid; maximum deviations of 4.9% for water and 5.8% for FC-77; $5000 \leqslant Re_D \leqslant 14\,000$; $5.4 \leqslant Pr \leqslant 28.1$; $T_w - T_b \leqslant 15^\circ C$; $H = 11.9$ mm; $W = 50.8$ mm; $W_q = 12.7$ mm; $L_q = 12.7$ mm; $D_h = 19.3$ mm.	11.2*
Maddox and Mudawar [19]	$\overline{Nu_L} = 0.0237 Re_L^{0.608}\, Pr^{1/3}$ (a)	Rectangular channel with short, discrete heater; properties at inlet temperature, except μ_w at T_w; developed with FC-72 liquid; (a) has mean absolute error of 3.5%; $4200 \leqslant Re_D \leqslant 2.2 \times 10^5$; $8.9 \leqslant Pr \leqslant 12.6$; $H = 12.7$ mm; $W = 38.1$ mm; $W_q = 12.7$ mm; $L_q = 12.7$ mm; $D_h = 19.1$ mm.	13.6*
	$\overline{Nu_L} = 0.18 Re_D^{0.64}\, Pr^{0.38} \left(\frac{\mu}{\mu_w}\right)^{0.25}$ (b)	"	43.5*
Samant and Simon [20]	$Nu_H = 0.47 Re_H^{0.58}\, Pr^{0.50}$	Rectangular channel with very short heater; properties at inlet temperature; developed with FC-72 and R-113 liquids; standard deviation of 5.6%; $9400 \leqslant Re_D \leqslant 2.4 \times 10^5$; $Pr \approx 10.0$; $H = 2.79$ mm; $W = 10.26$ mm; $W_q = 2.00$ mm; $L_q = 0.25$ mm; $D_h = 4.39$ mm.	41.4
Gersey and Mudawar [21]	$\overline{Nu_L} = 0.362 Re_L^{0.614}\, Pr^{1/3}$	Rectangular channel with short, discrete heater; properties at inlet temperature; developed with FC-72 liquid; based on 12 399 data points with mean absolute error of 5.1%; $2900 \leqslant Re_D \leqslant 1.6 \times 10^5$; $Pr = 10.0$; $H = 5.0$ mm; $W = 20.0$ mm; $W_q = 10.0$ mm; $L_q = 10.0$ mm; $D_h = 8.0$ mm.	17.4*

* Correlation recast with Nusselt and Reynolds numbers based on hydraulic diameter before comparison to present data.

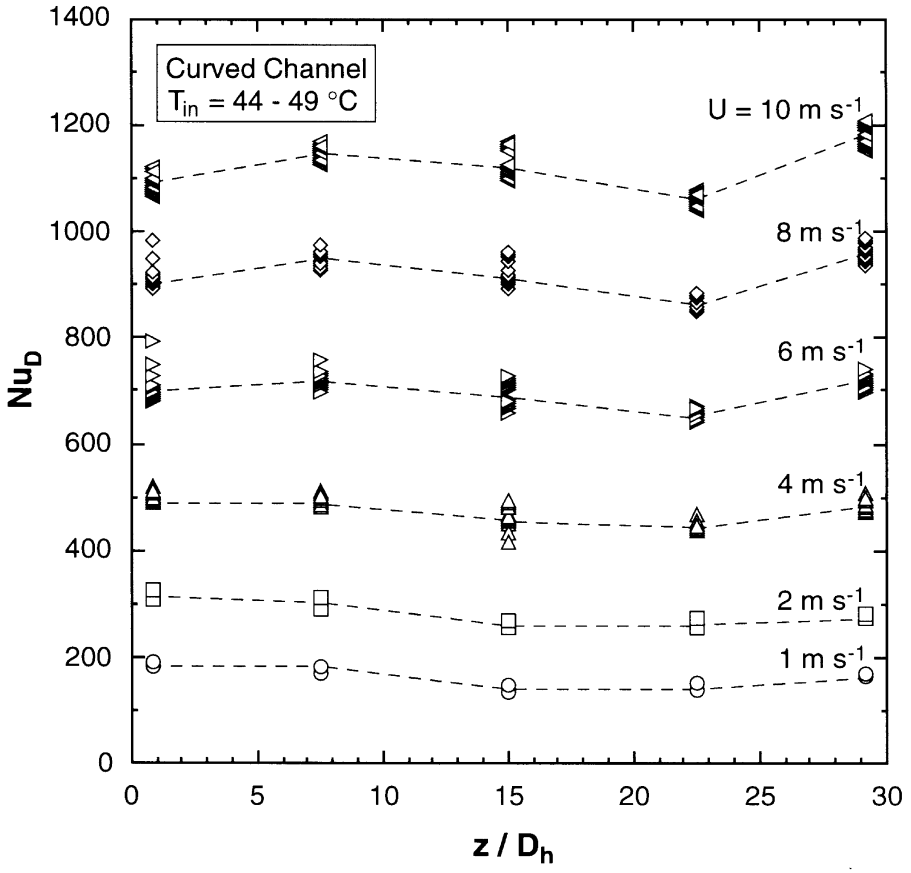

Fig. 8. Nusselt number variation along heated wall in curved channel.

with a mean absolute error of 3.9%; all properties were evaluated at the bulk temperature at Location 5. The Reynolds number exponent is greater than that for the straight correlation (eqn (7)) reflecting a stronger dependence on velocity and indicating that enhancement due to curvature increases with increasing velocity.

In their work with coiled tubes, Seban and McLaughlin [1] developed a correlation, based on a curved-to-straight-flow friction factor ratio by Ito [11], that accounts for this enhancement. They proposed

$$\overline{Nu_D} = 0.023 Re_D^{0.8}\, Pr^{0.4}\left[Re_D\left(\frac{D}{d_c}\right)^2\right]^{1/20} = 0.023 Re_D^{0.85}\, Pr^{0.4}\left(\frac{D}{d_c}\right)^{0.1} \quad (15)$$

where properties are evaluated at the film temperature, D is the tube diameter, and d_c the curvature (coil) diameter. Ito's relation is applicable for

$$Re_D\left(\frac{D_h}{d_c}\right)^2 > 6. \quad (16)$$

Considering the present study, $d_c/D_h = 19.1$ and $Re_D(D_h/d_c)^2 > 25$ for all the data.

Seban and McLaughlin's expression, essentially an augmentation of the Dittus–Boelter straight channel correlation, underpredicts the present data at the exit by 25%, as illustrated in Fig. 9. Rogers and Mayhew [2] arrived at the same equation with properties evaluated at the bulk temperature but offered no better prediction of the present data. Pratt [3] assumed an enhancement factor that depends only on geometry and from his data deduced this factor to be $[1+3.4(D/d_c)]$. All these investigations concern full-periphery-heated coiled tubes in which in some cases the convection coefficient varied by as much as a factor of four [1] between the outer wall of the cross-section (farther from the coil axis) and the inner wall. However, peripherally-averaged convection coefficients were used to develop these correlations which diluted the curvature enhancement effect. It is then understandable that these correlations underpredict the present concave-heated data. Therefore, the heating boundary condition—full-periphery or one-sided—is important in the selection of a curved correlation. Table 3 lists cor-

Table 3
Heat transfer correlations for flow in curved channels (I)

Location	Present curved channel correlations	Elaboration	Mean absolute error with respect to data at location (%)
1	$Nu_D = 0.0597 Re_D^{0.765}\, Pr^{0.4}$	Curved, rectangular channel with concave heating; properties at local bulk temperature; developed with FC-72 liquid; Nu_D based on local convection coefficient and hydraulic diameter; each correlation based on 474 data points covering $U = 1-10\ \mathrm{m\,s^{-1}}$; $d_c/D_h = 19.1$; $9000 \leqslant Re_D \leqslant 130\,000$; $8.5 \leqslant Pr \approx 11.2$; $3 \leqslant g^* \leqslant 315$.	5.2
2	$Nu_D = 0.0298 Re_D^{0.829}\, Pr^{0.4}$	”	5.9
3	$Nu_D = 0.0174 Re_D^{0.871}\, Pr^{0.4}$	”	2.8
4	$Nu_D = 0.0233 Re_D^{0.843}\, Pr^{0.4}$	”	5.0
5	$Nu_D = 0.0225 Re_D^{0.854}\, Pr^{0.4}$	”	3.9
Author [ref]	Published correlations (eqn)	Elaboration	Mean absolute error with respect to location 5 data (%)
Pratt [3]	$\overline{Nu_D} = 0.0225\left(1+3.4\dfrac{D}{d_c}\right) Re_D^{0.8}\, Pr^{0.4}$	Tubular coil with full-periphery heating; properties at bulk temperature; developed with water; $\overline{Nu_D}$ based on periphally-averaged convection coefficient; $d_c/D = 10$–23; $Re_D \geqslant 15\,000$–$20\,000$; $Pr \approx 3$.	34.5
Seban and McLaughlin [1]	$\overline{Nu_D} = 0.023 Re_D^{0.8}\, Pr^{0.4}\left[Re_D\left(\dfrac{D}{d_c}\right)^2\right]^{1/20}$	Tubular coil with full-periphery heating; properties at film temperature; developed with water; $\overline{Nu_D}$ based on periphally-averaged convection coefficient; utilizes Ito's [11] friction factor ratio; uncertainty of 10% for large coil ($d_c/D = 104$) and 15% for small coil ($d_c/D = 17$); $6000 \leqslant Re_D \leqslant 65\,000$; $2.9 \leqslant Pr \leqslant 5.7$.	24.8
Rogers and Mayhew [2]	$\overline{Nu_D} = C Re_D^{0.8}\, Pr^{0.4}\left[Re_D\left(\dfrac{D}{d_c}\right)^2\right]^{1/20}$ $C = 0.021$ for properties at film temperature	Tubular coil with full-periphery heating; developed with water; $\overline{Nu_D}$ based on periphally-averaged convection coefficient; utilizes Ito's [11] friction factor ratio; uncertainty of 10% for coils with $d_c/D = 10$–20; $3000 \leqslant Re_D \leqslant 50\,000$; $Pr \approx 3$.	31.3 (film)
	$C = 0.023$ for properties at bulk temperature	”	27.0 (bulk)
Mori and Nakayama [22]	$\overline{Nu_D} = \dfrac{1}{41} Re_D^{5/6}\, Pr^{0.4} \times \left(\dfrac{D}{d_c}\right)^{1/12}\left[1+\dfrac{0.061}{\left[Re_D\left(\dfrac{D}{d_c}\right)^{2.5}\right]^{1/6}}\right]$	Curved tube with full-periphery heating; properties at bulk temperature; developed mostly from a theoretical analysis for fully-developed turbulent flow ($Re_D \geqslant 10^4$) of liquids; $Pr > 1$.	29.9

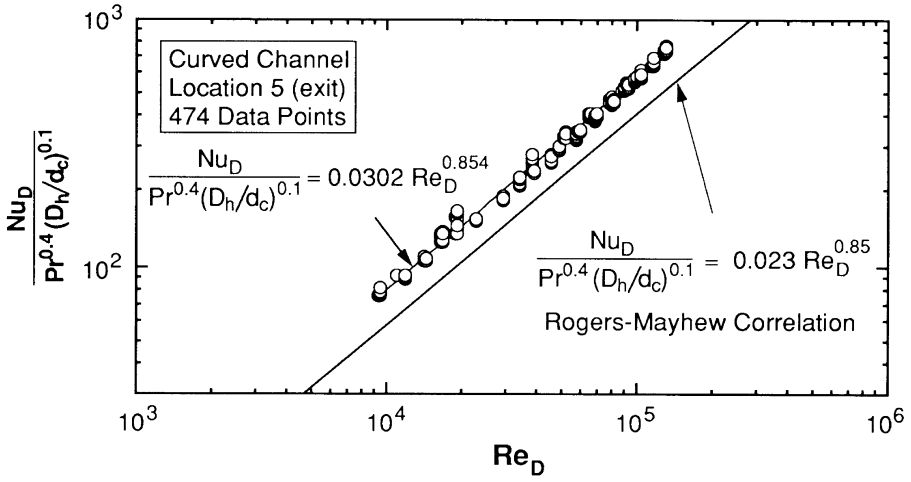

Fig. 9. Data and correlation for present curved, one-side-heated channel compared with Rogers–Mayhew correlation [2] for full-periphery-heated, coiled tubes.

relations applicable to heat transfer in curved passages with notes on their applicability and accuracy in predicting the present data at the heater exit.

Nusselt number data in the curved channel may also be redefined with different length scales resulting in trends similar to those observed for the straight channel case. As before, Nusselt numbers defined using thermal diameter are significantly underpredicted. When heated width, W, is used, the data are represented well by the Rogers–Mayhew correlation though the agreement is circumstantial due to the particular value of width and the use of inconsistent length scales. Since data may be defined in numerous ways, correlations must therefore be used with caution when applied to curved, partial-periphery-heated passages.

Data at the exit of the curved channel, though not confirmed to be thermally fully-developed, are correlated using heated width by the expression

$$Nu_w = \frac{hW}{k} = 0.0169 Re_D^{0.854} Pr^{0.4} = 0.0227 Re_D^{0.854} Pr^{0.4} \left(\frac{D_h}{2R_2}\right)^{0.1}. \quad (17)$$

4. Enhancement mechanisms

Prior to comparing straight and curved data to evaluate the enhancement due to streamwise curvature, the characteristics of curved flow responsible for this enhancement are discussed. For the flow of fluid in a curved passage, the interaction between pressure, viscous and inertial forces leads to secondary motion known as Dean vortices, illustrated in Fig. 10(a). As the fluid moves through the curved section, a radial pressure gradient is established, with pressure increasing radially outward, which turns the fluid particles along the channel path. The motion of the fluid in the vicinity of the side walls is retarded by viscous forces and this low momentum fluid, in the presence of the pressure gradient, is forced toward the inner wall. Meanwhile, the fluid in the center of the channel, experiencing no appreciable resistance to motion, moves toward the outer wall due to its inertia [23]. Thus, the outward motion of fluid in the center of the channel and the inward motion of fluid near the side walls comprise a secondary motion, which when superimposed on the axial bulk flow, creates the counter-rotating vortices characteristic of flows in curved channels. Dean [24] developed an analytical expression that revealed this secondary motion for flow in pipes with mild curvature. The basic configuration is one pair of counter-rotating vortices although for large Reynolds numbers and large width-to-height ratio channels additional pairs may develop [25].

One parameter which characterizes the degree to which these secondary flows are present is the Dean number, defined in Table 1. It represents the ratio of the square root of the product of inertial and centrifugal (pressure) forces to the viscous forces [23]. The effect of secondary flows is much greater for turbulent flow as indicated by a larger Dean number [9].

In addition to the Dean vortices, numerical analyses [26] and experiments [9] have shown a shift in the location of the maximum axial velocity for curved flow, shown by the velocity contours and profiles in Fig. 10(b). This results in a higher velocity gradient, and shear stress, at the outer wall when compared with a straight duct.

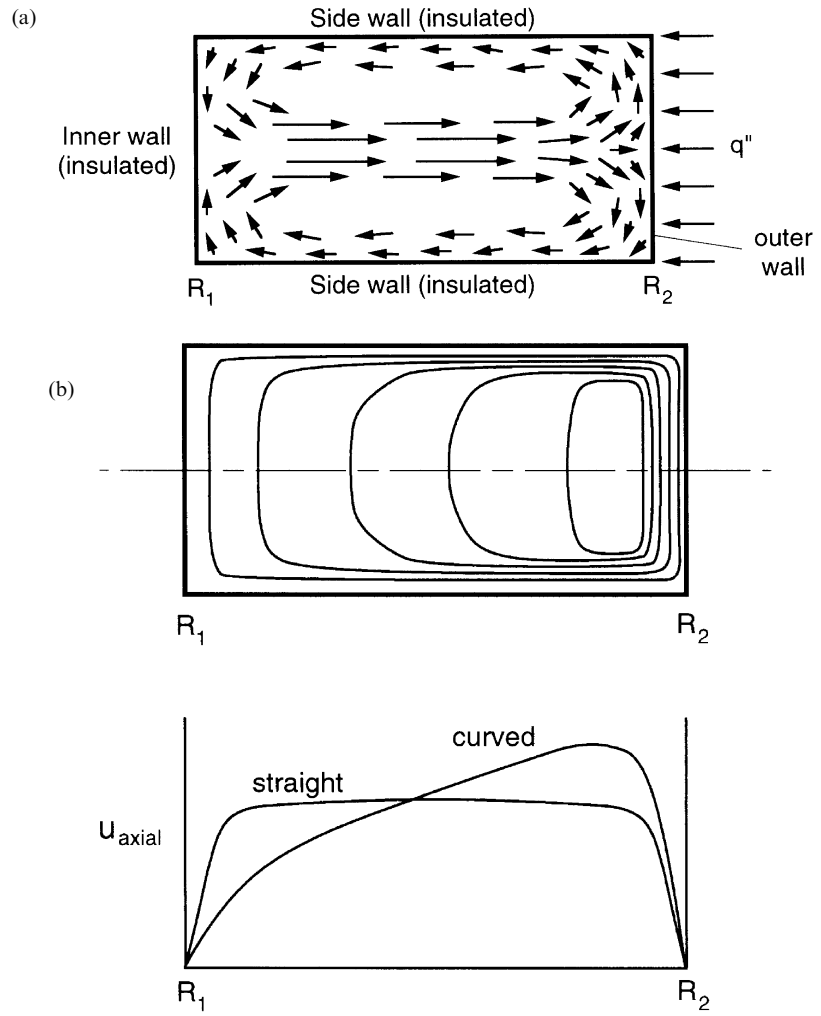

Fig. 10. Heat transfer enhancement mechanisms: (a) Dean vortices; (b) shift in location of maximum axial velocity toward outer (heated) wall.

Therefore, the primary mechanisms for increasing the convection coefficient in a curved channel over that in a straight channel (which will be demonstrated in the next section) must also be the *Dean vortices* and the *maximum velocity shift* toward the outer wall. The vortex pair moves warmer fluid away from the concave surface and replaces it with cooler fluid. This thermal mixing, along with the maximum velocity shift, enables the cooler bulk fluid to exist closer to the heated wall thereby reducing the thermal boundary layer thickness and thermal resistance, in other words, enhancing heat transfer.

5. Enhancement ratio

Comparison of straight and curved channel data indicates higher convection coefficients for curved flow, the enhancement being, on average, 12% for $U = 2$ m s^{-1}, 23% for $U = 6$ m s^{-1} and 26% for $U = 10$ m s^{-1}.

The enhancement ratio associated with the present data was ascertained by rewriting the curved correlation (eqn (14)) to include the geometrical parameters of the curved channel. Doing so and recalling eqn (7) for the straight channel yields

$$Nu_{D,\mathrm{cur}} = 0.0225 Re_D^{0.854} Pr^{0.4} = 0.0302 Re_D^{0.808} Pr^{0.4} \left[Re_D^{0.046} \left(\frac{D_h}{2R_2} \right)^{0.1} \right], \quad (18)$$

$$\frac{Nu_{D,\mathrm{cur}}}{Nu_{D,\mathrm{str}}} \approx Re_D^{0.046} \left(\frac{D_h}{2R_2} \right)^{0.1}. \quad (19)$$

The enhancement ratio given by eqn (19) is similar to the ratio proposed by Seban and McLaughlin [1], eqn (15),

and supported by Rogers and Mayhew [2] for bulk temperature properties. The ratios differ by only 6% over the applicable range of Reynolds number due to the slight difference tin the Re_D exponent.

The ratios of curved-to-straight channel Nusselt numbers based on the correlations developed from the present data are plotted in Fig. 11 against Re_D. The ratios for Locations 2–5 are those curved channel correlations specific to each of these locations (see Table 3) divided by the thermally fully-developed correlation of the straight channel (see eqn (7)). For Location 1, Fig. 11 shows the ratio of Location 1 correlations for the respective channels. Also plotted are the enhancement ratios of Rogers and Mayhew and Pratt.

Figure 11 shows that for locations downstream of the inlet (Locations 2–5), the enhancement due to curvature increases with increasing Re_D since the secondary flows become more pronounced as mean velocity and Dean number increase [9]. The ratio for Location 1 is interesting since it reveals that curvature becomes less significant (enhancement decreasing from about 14 to 4%) as Reynolds number increases. The trend can be explained as follows. As the streamwise momentum of fluid entering the curved section increases for increasing Reynolds number, the flow is less likely to be hydrodynamically influenced by the short segment upstream of the first location. That is, the ability of this short curved region upstream of Location 1 to communicate its resistance to the bulk flow diminishes as the flow's momentum increases; therefore, the flow over this short length at the inlet tends to behave more like straight-channel flow. Hence, as Reynolds number increases, heat transfer characteristics also tend toward those of straight-channel flow, which is reflected in the reduction of enhancement ratio toward unity at the inlet. However, increasing the Reynolds number does not yield similar results at the downstream locations since, by the time the flow reaches Location 2 ($\theta = 45^\circ$), Dean vortices are forming and the maximum axial velocity is shifting toward the concave wall [6]. These contribute to significant enhancement even at low Re_D for Location 2.

Enhancement ratios for Locations 2–5 range from 2 to 18% at $Re_D = 10^4$ and from 14 to 25% at $Re_D = 10^5$. Locations 2 and 5 yielded, on average, the highest enhancement ratios, approximately 22%. Interestingly, Frohlich et al. [27] noted that rocket engine cooling designs usually allow for a 30% enhancement of the convection coefficient on the concave wall in the throat region, where Reynolds number is higher than in the present data.

Figure 11 shows that the enhancement ratio of Rogers and Mayhew [2] reflects the trend of enhancement increasing with Reynolds number while the *Re*-independent enhancement ratio of Pratt does not. The ratio of Rogers and Mayhew overpredicts the enhancement over nearly the entire Reynolds number range though the slope (Reynolds number exponent, 0.05) is similar to the slopes for Locations 4 and 5, which are 0.035 and 0.046, respectively. From the similarity of Reynolds number exponents in the present downstream enhancement ratios (Locations 4 and 5), it appears the curved channel flow is becoming fully-developed and approaching a single expression for enhancement. In the present study, the ratio of heated length to hydraulic diameter is 30, whereas in the experiments of Seban and McLaughlin [1] and Rogers and Mayhew the shortest tube used was over

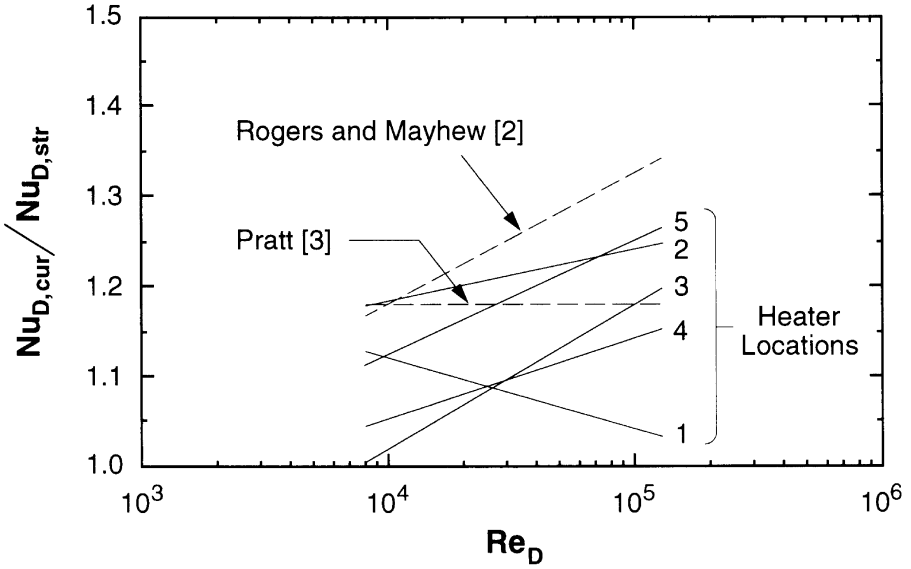

Fig. 11. Ratio of curved-to-straight-channel Nusselt numbers based on data and published correlations.

270 diameters long. This contrast in heated length may explain the differences, especially upstream. Also, the use of peripherally-averaged convection coefficients (even though heat transfer varies greatly around the perimeter) influences the ratio between curved and straight channel Nusselt numbers.

6. Conclusions

This paper describes an investigation into single-phase heat transfer for turbulent flow in curved and straight rectangular channels subjected to one-sided heating, with the curved channel subjected to concave heating. Correlations were developed and Nusselt numbers compared to assess the enhancement due to curvature. Key conclusions from this study are as follows:

(1) The heat transfer coefficient in the straight channel increases with increasing velocity and thermally fully-developed conditions are attained by $z/D_h \approx 8$. Nusselt numbers for the thermally fully-developed region correlate well with Reynolds number to the 0.808 power, similar to the dependence given by the Dittus–Boelter correlation. However, straight channel Nusselt numbers defined with hydraulic, D_h, or thermal, D_{th}, diameters are consistently underpredicted by the Dittus–Boelter correlation which was developed for full periphery-heated tubes. Nusselt numbers defined with heated width, W, are represented well by the Dittus–Boelter correlation though no significance is attributed to this agreement.

(2) The heat transfer in the curved channel increases with increasing velocity but thermally fully-developed conditions are not attained even at the exit of the heated curved section. Nusselt numbers for the exit of the curved channel are consistently underpredicted by the Rogers–Mayhew correlation when Nusselt number is defined with hydraulic or thermal diameters. The data are better predicted when Nusselt number is defined with heated width, though this is not considered meaningful since inconsistent definitions are employed between the data and correlation.

(3) Increasing Reynolds number produces different enhancement trends for different locations along the heated wall, decreasing the enhancement near the inlet, where the effect of wall curvature is not yet felt by the flow, and increasing it elsewhere downstream. Mechanisms responsible for the downstream enhancement are Dean vortices and a shift in the maximum axial velocity toward the concave wall. These require a finite distance to develop sufficient strength to influence heat transfer, which explains the different enhancement trends observed for different locations along the heated wall.

(4) The full-periphery-heated tube enhancement ratio proposed by Seban and McLaughlin and modified by Rogers and Mayhew yields fair approximations of the present one-side-heated channel data.

Acknowledgements

The authors are grateful for the support of the Office of Basic Energy Sciences of the U.S. Department of Energy (Grant No. DE-FG02-93ER14394.A003). Financial support for the first author was provided through the Air Force Palace Knight Program.

References

[1] R.A. Seban, E.F. McLaughlin, Heat transfer in coiled tubes with laminar and turbulent flow, International Journal of Heat and Mass Transfer 6 (1963) 387–395.
[2] G.F.C. Rogers, Y.R. Mayhew, Heat transfer and pressure loss in helically coiled tubes with turbulent flow, International Journal of Heat and Mass Transfer 7 (1964) 1207–1216.
[3] N.H. Pratt, The heat transfer in a reaction tank cooled by means of a coil, Transactions of the Institution of Chemical Engineers 25 (1947) 163–180.
[4] P.D. McCormack, H. Welker, M. Kelleher, Taylor–Goertler vortices and their effect on heat transfer, ASME–AIChE Heat Transfer Conference, paper 69-HT-3, Minneapolis, MN, 1969.
[5] K.V. Dement'eva, I.Z. Aronov, Hydrodynamics and heat transfer in curvilinear channels of rectangular cross section (translated from Inzhernerno-Fizicheskii Zhurnal), Scientific-Research Institute of Sanitary Engineering, Equipment and Construction 34 (6) (1978) 994–1000.
[6] J.H. Chung, J.M. Hyun, Convective heat transfer in the developing flow region of a square duct with strong curvature, International Journal of Heat and Mass Transfer 35 (1992) 2537–2550.
[7] J.G. Collier, J.R. Thome, Convective Boiling and Condensation, 3rd ed., Clarendon Press, Oxford, 1994.
[8] W.M. Kays, H.C. Perkins, Forced convection, internal flow in ducts, in: W.M. Rohsenow, J.P. Hartnett (Eds.), Handbook of Heat Transfer, McGraw-Hill, Inc., New York, 1973.
[9] J.A.C. Humphrey, J.H. Whitelaw, G. Yee, Turbulent flow in a square duct with strong curvature, Journal of Fluid Mechanics 103 (1981) 443–463.
[10] E. Baker, Liquid cooling of microelectronic devices by free and forced convection, Microelectronics and Reliability 11 (1972) 213–222.
[11] H. Ito, Friction factors for turbulent flow in curved pipes, ASME Journal of Basic Engineering (1959) 123–134.
[12] J.P.Hartnett, Experimental determination of the thermal-entrance length for the flow of water and or oil in circular pipes, ASME Journal of Heat Transfer 77 (1955) 211–1220.

[13] W.M. Kays, M.E. Crawford, Convective Heat and Mass Transfer, 2nd ed., McGraw-Hill, Inc., New York, 1980.
[14] F.W. Dittus, L.M.K. Boelter, Heat transfer in automobile radiators of the tubular type, University of California Publications in Engineering 2 (1930) 443–461.
[15] E. Choi, Y.I. Cho, Local friction and heat transfer behavior of water in a turbulent pipe flow with a large heat flux at the wall, ASME Journal of Heat Transfer 117 (1995) 283–288.
[16] E.N. Sieder, G.E. Tate, Heat transfer and pressure drop of liquids in tubes, Industrial and Engineering Chemistry 28 (1936) 1429–1435.
[17] B.S. Petukhov, V.N. Popov, Theoretical calculation of heat exchange and frictional resistance in turbulent flow in tubes of an incompressible fluid with variable physical properties (translated from Russian), High Temperature 1 (1963) 69–83.
[18] F.P. Incropera, J.S. Kerby, D.F. Moffatt, S. Ramadhyani, Convection heat transfer from discrete heat sources in a rectangular channel, International Journal of Heat and Mass Transfer 29 (1986) 1051–1058.
[19] D.E. Maddox, I. Mudawar, Single- and two-phase convective heat transfer from smooth and enhanced microelectronic heat sources in a rectangular channel, ASME Journal of Heat Transfer 111 (1989) 1045–1052.
[20] K.R. Samant, T.W. Simon, Heat transfer from a small heated region to R-113 and FC-72, ASME Journal of Heat Transfer 111 (1989) 1053–1059.
[21] C.O. Gersey, I. Mudawar, Effects of orientation on critical heat flux from chip arrays during flow boiling, ASME Journal of Electronic Packaging 114 (1992) 290–299.
[22] Y. Mori, W. Nakayama, Study on forced convective heat transfer in curved pipes (2nd report, turbulent region), International Journal of Heat and Mass Transfer 10 (1967) 37–59.
[23] S.A. Berger, L. Talbot, L.S. Yao, Flow in curved pipes, Annual Review of Fluid Mechanics 15 (1983) 461–512.
[24] W.R. Dean, Note on the motion of fluid in a curved pipe, The London, Edinburgh, and Dublin Philosophical Magazine and Journal of Science 6 (1927) 208–223.
[25] I.A. Hunt, P.N. Joubert, Effects of small streamline curvature on turbulent duct flow, Journal of Fluid Mechanics 91 (1979) 633–659.
[26] R.M. Eason, Y. Bayazitoglu, A. Meade, Enhancement of heat transfer in square helical ducts, International Journal of Heat and Mass Transfer 37 (1994) 2077–2087.
[27] A. Frohlich, H. Immich, F. LeBail, M. Popp, G. Scheuerer, Three-dimensional flow analysis in a rocket engine coolant channel of high depth/width ratio, AIAA/SAE/ASME/ASEE 27th Joint Propulsion Conference, Sacramento, CA, 1991.